Uplink Performance Analysis of Multicell MU-MIMO Systems with ZF Receivers

Hien Quoc Ngo, Michail Matthaiou, Trung Q. Duong, and Erik G. Larsson

Abstract

We consider the uplink of a multicell multiuser multiple-input multiple-output system where the channel experiences both small and large-scale fading. The data detection is done by using the linear zero-forcing technique, assuming the base station (BS) has perfect channel state information. We derive new, exact closed-form expressions for the uplink rate, symbol error rate, and outage probability per user, as well as a lower bound on the achievable rate. This bound is very tight and becomes exact in the large-number-of-antennas limit. We further study the asymptotic system performance in the regimes of high signal-to-noise ratio (SNR), large number of antennas, and large number of users per cell. We show that at high SNRs, the system is interference-limited and hence, we cannot improve the system performance by increasing the transmit power of each user. Instead, by increasing the number of BS antennas, the effects of interference and noise can be reduced, thereby improving the system performance. We demonstrate that, with very large antenna arrays at the BS, the transmit power of each user can be made inversely proportional to the number of BS antennas while maintaining a desired quality-of-service. Numerical results are presented to verify our analysis.

Index Terms

Multiuser MIMO, very large MIMO systems, zero-forcing receiver.

- H. Q. Ngo and E. G. Larsson are with the Department of Electrical Engineering (ISY), Linköping University, 581 83 Linköping, Sweden (email: nqhien@isy.liu.se; egl@isy.liu.se).
- M. Matthaiou is with the Department of Signals and Systems, Chalmers University of Technology, 412 96, Gothenburg, Sweden (email: michail.matthaiou@chalmers.se).
 - T. Q. Duong is with the Blekinge Institute of Technology 371 79, Karlskrona, Sweden (email: quang.trung.duong@bth.se).

The work of H. Q. Ngo and E. G. Larsson was supported in part by the Swedish Research Council (VR), the Swedish Foundation for Strategic Research (SSF), and ELLIIT. E. G. Larsson is a Royal Swedish Academy of Sciences (KVA) Research Fellow supported by a grant from the Knut and Alice Wallenberg Foundation. The work of M. Matthaiou was supported in part by the Swedish Governmental Agency for Innovation Systems (VINNOVA) within the VINN Excellence Center Chase.

Parts of this work were presented at the 2011 IEEE Swedish Communication Technologies Workshop [1].

I. Introduction

Multiple-input multiple-output (MIMO) technology can provide a remarkable increase in data rate and reliability compared to single-antenna systems. Recently, multiuser MIMO (MU-MIMO), where the base stations (BSs) are equipped with multiple antennas and communicate with several co-channel users, has gained much attention and is now being introduced in several new generation wireless standards (e.g., LTE-Advanced, 802.16m) [2].

MU-MIMO systems have been studied from many perspectives including communication, signalling, and information theory in both downlink and uplink scenarios [3], [4]. For the uplink, the maximum-likelihood multiuser detector can be used to obtain optimal performance [5]. However, this optimum receiver induces a significant complexity burden on the system implementation, especially for large array configurations. Therefore, linear receivers, in particular Zero-Forcing (ZF) receivers, are of particular interest as low-complexity alternatives [6]–[8]. Note that all the above mentioned works have only investigated a single-cell scenario, where the effects of intercell interference have been neglected. However, co-channel interference, appearing due to frequency-reuse, represents an important impairment in cellular systems. Recently, there has been an increasing research interest in the performance of MU-MIMO in interference-limited multi-cell environments [9]–[13]. In fact, it has been shown that the capacity of the MU-MIMO downlink can be dramatically reduced due to intercell interference [9].

Mu-MIMO systems, such as maximum likelihood multiuser detection [11], BS cooperation [14], and interference alignment [15]. These techniques, however, have a high implementation complexity. Very recently, there has been a great deal of interest in multicell MU-MIMO, where the BSs are equipped with very large antenna arrays [16]–[20]. With very large antenna arrays, the intercell interference can be successfully handled by using simple linear detectors, because the channel vectors are nearly orthogonal when the number of antennas is large (see e.g., [16], [19] for a more detailed discussion). In this context, the asymptotic signal-to-interference-plusnoise ratios (SINRs), when the number of BS antennas grows infinite, were derived in [17] for maximum-ratio combining (MRC) in the uplink and maximum-ratio transmission in the downlink. In [20], by using tools of random matrix theory, the authors derived a deterministic approximation of the SINR for the uplink with MRC and minimum mean-square error (MMSE) receivers, assuming that the number of transmit antennas and number of users go to infinity at

the same rate. They also showed that the deterministic approximation of the SINR is tight even with a moderate number of BS antennas and users. However, since the limiting SINR obtained therein is deterministic, this approximation does not enable us to further analyze other figures of merit, such as the outage probability or symbol error rate (SER). More importantly, iterative algorithms are needed to compute the deterministic equivalent results. In [19], lower bounds on the uplink achievable rates with linear detectors were computed, and the authors showed that MRC performs as well as ZF in a regime where the spectral efficiency is of the order of 1 bpcu per user. Nevertheless, it was demonstrated that ZF performs much better than MRC at higher spectral efficiencies.

Inspired by the above discussion, we analyze in this paper the performance of multicell MU-MIMO systems where many users simultaneously transmit data to a BS. The BS uses ZF to detect the transmitted signals. Note that the MMSE receiver always performs better than the ZF receiver. However, herein we consider ZF receivers for the following reasons: i) an exact analysis of MMSE receivers is a challenging mathematical problem in a multicell MU-MIMO setup. This implication can be seen by invoking the generic results of [21]; ii) the implementation of MMSE receivers requires additional knowledge of the noise and interference statistics; iii) it is well-known that ZF receivers perform equivalently to MMSE receivers at high SNIRs [22]; and iv) the performance of ZF bounds that of MMSE from below, so the results we obtain represent achievable lower bounds on the MMSE receivers' performance. The paper makes the following specific contributions:

- We derive exact closed-form expressions for the ergodic data rate, SER, and outage probability of the uplink channel for any finite number of BS antennas. We also derive a tractable lower bound on the achievable rate. Note that, although these exact results involve complicated functions, they can be much more efficiently evaluated compared to brute-force Monte-Carlo simulations.
- Next, we focus on the ZF receiver's asymptotic performance when the BS deploys a large antenna array. These results enable us to explicitly study the effects of transmit power, intercell interference, and number of BS antennas. For instance, when the number of users per cell is fixed and the number of BS antennas grows without bound, intercell interference and noise are averaged out. However, when fixing the ratio between the number of BS antennas and the number of users, the intercell interference does not vanish when the

number of antennas grows large. Yet, in both cases by using very large antenna arrays, the transmit power of each user can be made inversely proportional to the number of antennas with no performance degradation.

Notation: The superscript H stands for conjugate transpose. $[A]_{ij}$ denotes the (i,j)th entry of a matrix A, and I_n is the $n \times n$ identity matrix. The expectation operation and the Euclidean norm are denoted by $\mathbb{E}\left\{\cdot\right\}$ and $\|\cdot\|$, respectively. The notation $\stackrel{\text{a.s.}}{\to}$ means almost sure convergence. We use $a \stackrel{\text{d}}{=} b$ to imply that a and b have the same distribution. Finally, we use $z \sim \mathcal{CN}\left(\mathbf{0}, \mathbf{\Sigma}\right)$ to denote a circularly symmetric complex Gaussian vector z with zero-mean and covariance matrix $\mathbf{\Sigma}$.

II. MULTICELL MU-MIMO SYSTEM

In the following, we consider a multicell MU-MIMO system with L cells. Each cell includes one BS equipped with N antennas, and K single-antenna users ($N \ge K$). We consider uplink transmission, and assume that the L BSs share the same frequency band. Conventionally, the communication between the BS and the users is performed in separate time-frequency resources. However, this approach inherently reduces the spectral efficiency and it is therefore more efficient if several users communicate with the BS in the same time-frequency resource [13], [17]. We assume that all users simultaneously transmit data streams to their BSs. Therefore, the $N \times 1$ received vector at the lth BS is given by

$$\boldsymbol{y}_l = \sqrt{p_{\mathrm{u}}} \sum_{i=1}^{L} \boldsymbol{G}_{li} \boldsymbol{x}_i + \boldsymbol{n}_l \tag{1}$$

where $G_{li} \in \mathbb{C}^{N \times K}$ is the channel matrix between the lth BS and the K users in the ith cell, i.e., $g_{limk} \triangleq [G_{li}]_{mk}$ is the channel coefficient between the mth antenna of the lth BS and the kth user in the ith cell; $\sqrt{p_{\rm u}} \boldsymbol{x}_i \in \mathbb{C}^{K \times 1}$ is the transmitted vector of K users in the ith cell (the average power transmitted by each user is $p_{\rm u}$); and $\boldsymbol{n}_l \in \mathbb{C}^{N \times 1}$ is an additive white Gaussian noise (AWGN) vector, such that $\boldsymbol{n}_l \sim \mathcal{CN}\left(\mathbf{0}, \boldsymbol{I}_M\right)$. Note that, since the noise power is assumed to be 1, $p_{\rm u}$ can be considered as the normalized "transmit" SNR and hence, it is dimensionless.

The channel matrix, G_{li} , models independent fast fading, path-loss attenuation, and log-normal shadow fading. The assumption of independent fast fading is sufficiently realistic for systems where the antennas are sufficiently well separated [23]. Hence, its elements g_{limk} are given by

$$g_{limk} = h_{limk} \sqrt{\beta_{lik}}, \quad m = 1, 2, ..., N$$
 (2)

where h_{limk} is the fast fading coefficient from the kth user in the ith cell to the mth antenna of the lth BS. The coefficient h_{limk} is assumed to be complex Gaussian distributed with zeromean and unit variance. Moreover, $\sqrt{\beta_{lik}}$ represents the path-loss attenuation and shadow fading which are assumed to be independent over m and to be constant over many coherent intervals. This assumption is reasonable since the distance between users and the BS is much greater than the distance between the BS antennas. Additionally, the validity of this assumption has been demonstrated in practice even for large antenna arrays [24].

We assume that the BS has perfect channel state information (CSI). This assumption is reasonable in an environment with low or moderate mobility, so that long training intervals can be afforded. Moreover, the results obtained under this assumption serve as bounds on the performance for the case that the CSI is imperfect due to estimation errors or feedback delays. We further assume that the transmitted signals from the K users in the lth cell are detected using a ZF receiver. As such, the received vector \mathbf{y}_l is processed by multiplying it with the pseudo-inverse of \mathbf{G}_{ll} as:

$$\boldsymbol{r}_{l} = \boldsymbol{G}_{ll}^{\dagger} \boldsymbol{y}_{l} = \sqrt{p_{\mathrm{u}}} \boldsymbol{x}_{l} + \sqrt{p_{\mathrm{u}}} \sum_{i \neq l}^{L} \boldsymbol{G}_{ll}^{\dagger} \boldsymbol{G}_{li} \boldsymbol{x}_{i} + \boldsymbol{G}_{ll}^{\dagger} \boldsymbol{n}_{l}$$
(3)

where $\boldsymbol{G}_{ll}^{\dagger} \triangleq \left(\boldsymbol{G}_{ll}^{H}\boldsymbol{G}_{ll}\right)^{-1}\boldsymbol{G}_{ll}^{H}$. Therefore, the kth element of \boldsymbol{r}_{l} is given by

$$\boldsymbol{r}_{l,k} = \sqrt{p_{\mathrm{u}}}\boldsymbol{x}_{l,k} + \sqrt{p_{\mathrm{u}}}\sum_{i\neq l}^{L} \left[\boldsymbol{G}_{ll}^{\dagger}\right]_{k} \boldsymbol{G}_{li}\boldsymbol{x}_{i} + \left[\boldsymbol{G}_{ll}^{\dagger}\right]_{k} \boldsymbol{n}_{l}$$
 (4)

where $x_{l,k}$ is the kth element of x_l , which is the transmitted signal from the kth user in the lth cell, while $[A]_k$ denotes the kth row of a matrix A. From (4), the SINR of the uplink transmission from the kth user in the lth cell to its BS is defined as

$$\gamma_{k} \triangleq \frac{p_{\mathrm{u}}}{p_{\mathrm{u}} \sum_{i \neq l}^{L} \left\| \left[\boldsymbol{G}_{ll}^{\dagger} \right]_{k} \boldsymbol{G}_{li} \right\|^{2} + \left\| \left[\boldsymbol{G}_{ll}^{\dagger} \right]_{k} \right\|^{2}}.$$
 (5)

Proposition 1: The SINR of the uplink transmission from the kth user in the lth cell to its BS can be represented as

$$\gamma_k \stackrel{\text{d}}{=} \frac{p_{\mathbf{u}} X_k}{p_{\mathbf{u}} Z_l + 1} \tag{6}$$

where X_k and Z_l are independent random variables (RVs) whose probability density functions (PDFs) are respectively given by

$$p_{X_k}(x) = \frac{e^{-x/\beta_{llk}}}{(N-K)!\beta_{llk}} \left(\frac{x}{\beta_{llk}}\right)^{N-K}, \ x \ge 0$$

$$(7)$$

$$p_{Z_l}(z) = \sum_{m=1}^{\varrho(\mathcal{A}_l)} \sum_{n=1}^{\tau_m(\mathcal{A}_l)} \mathcal{X}_{m,n}(\mathcal{A}_l) \frac{\mu_{l,m}^{-n}}{(n-1)!} z^{n-1} e^{\frac{-z}{\mu_{l,m}}}, \quad z \ge 0$$
 (8)

where $A_l \in \mathbb{C}^{K(L-1) \times K(L-1)}$ is given by

and $\varrho(\mathcal{A}_l)$ is the number of distinct diagonal elements of \mathcal{A}_l ; $\mu_{l,1}, \mu_{l,2}, ..., \mu_{l,\varrho(\mathcal{A}_l)}$ are the distinct diagonal elements in decreasing order; $\tau_m(\mathcal{A}_l)$ is the multiplicity of $\mu_{l,m}$; and $\mathcal{X}_{m,n}(\mathcal{A}_l)$ is the (m,n)th characteristic coefficient of \mathcal{A}_l which is defined in [27, Definition 4].

Proof: Dividing the denominator and nominator of (5) by $\|[G_{ll}^{\dagger}]_{k}\|^{2}$, we obtain

$$\gamma_k = \frac{p_{\mathrm{u}} \left\| \left[\boldsymbol{G}_{ll}^{\dagger} \right]_k \right\|^{-2}}{p_{\mathrm{u}} \sum_{i \neq l}^{L} \left\| \boldsymbol{Y}_i \right\|^2 + 1}$$
(9)

where $\boldsymbol{Y}_{i} \triangleq \frac{\left[\boldsymbol{G}_{ll}^{\dagger}\right]_{k}\boldsymbol{G}_{li}}{\left\|\left[\boldsymbol{G}_{ll}^{\dagger}\right]_{k}\right\|^{2}}$. Since $\left\|\left[\boldsymbol{G}_{ll}^{\dagger}\right]_{k}\right\|^{2} = \left[\left(\boldsymbol{G}_{ll}^{H}\boldsymbol{G}_{ll}\right)^{-1}\right]_{kk}$, $\left\|\left[\boldsymbol{G}_{ll}^{\dagger}\right]_{k}\right\|^{-2}$ has an Erlang distribution with shape parameter N-K+1 and scale parameter β_{llk} [28]. Then,

$$\left\| \left[\mathbf{G}_{ll}^{\dagger} \right]_{k} \right\|^{-2} \stackrel{\mathrm{d}}{=} X_{k}. \tag{10}$$

Conditioned on $\left[\boldsymbol{G}_{ll}^{\dagger}\right]_{k}$, \boldsymbol{Y}_{i} is a zero-mean complex Gaussian vector with covariance matrix \boldsymbol{D}_{li} which is independent of $\left[\boldsymbol{G}_{ll}^{\dagger}\right]_{k}$. Therefore, $\boldsymbol{Y}_{i} \sim \mathcal{CN}\left(\mathbf{0}, \boldsymbol{D}_{li}\right)$, where \boldsymbol{D}_{li} is a $K \times K$ diagonal matrix whose elements are given by $\left[\boldsymbol{D}_{li}\right]_{kk} = \beta_{lik}$. Then, $\sum_{i \neq l}^{L} \|\boldsymbol{Y}_{i}\|^{2}$ is the sum of K(L-1) statistically independent but not necessarily identically distributed exponential RVs. Thus, from [29, Theorem 2], we have that

$$\sum_{i \neq l}^{L} \|\boldsymbol{Y}_i\|^2 \stackrel{\mathrm{d}}{=} Z_l. \tag{11}$$

From (9)–(11), we can obtain (6).

III. FINITE-N ANALYSIS

In this section, we present exact analytical expressions for the ergodic uplink rate, SER, and outage probability of the system described in Section II. We underline the fact that the following results hold for any arbitrary number of BS antennas $N \ge K$.

A. Uplink Rate Analysis

From Proposition 1, the uplink ergodic rate from the kth user in the lth cell to its BS (in bits/s/Hz) is given by

$$\langle R_{k} \rangle = \mathbb{E}_{X_{k},Z_{l}} \left\{ \log_{2} \left(1 + \frac{p_{u}X_{k}}{p_{u}Z_{l} + 1} \right) \right\} = \int_{0}^{\infty} \int_{0}^{\infty} \ln \left(1 + \frac{p_{u}x}{p_{u}z + 1} \right) p_{X_{k}}(x) p_{Z_{l}}(z) dxdz$$

$$= \sum_{m=1}^{\varrho(\mathcal{A}_{l})} \sum_{n=1}^{\tau_{m}(\mathcal{A}_{l})} \frac{\mathcal{X}_{m,n}(\mathcal{A}_{l}) \mu_{l,m}^{-n} \log_{2} e}{(n-1)! (N-K)! \beta_{llk}^{N-K+1}} \int_{0}^{\infty} \int_{0}^{\infty} \ln \left(1 + \frac{p_{u}x}{p_{u}z + 1} \right) x^{N-K} e^{\frac{-x}{\beta_{llk}}} z^{n-1} e^{\frac{-z}{\mu_{l,m}}} dxdz. \quad (12)$$

We first evaluate the integral over x. By using [30, Eq. (4.337.5)], we obtain

$$\langle R_{k} \rangle = \sum_{m=1}^{\varrho(\mathcal{A}_{l})} \sum_{n=1}^{\tau_{m}(\mathcal{A}_{l})} \sum_{p=0}^{N-K} \frac{\mathcal{X}_{m,n} (\mathcal{A}_{l}) \mu_{l,m}^{-n} \log_{2} e}{(n-1)! (N-K-p)!} \int_{0}^{\infty} \left[\frac{-(p_{u}z+1)^{N-K-p}}{(-\beta_{llk}p_{u})^{N-K-p}} e^{\frac{p_{u}z+1}{\beta_{llk}p_{u}}} \operatorname{Ei} \left(-\frac{p_{u}z+1}{\beta_{llk}p_{u}} \right) + \sum_{q=1}^{N-K-p} (q-1)! \left(-\frac{p_{u}z+1}{\beta_{llk}p_{u}} \right)^{N-K-p-q} \right] z^{n-1} e^{-z/\mu_{l,m}} dz$$
(13)

where $\text{Ei}\left(\cdot\right)$ is the exponential integral function [30, Eq. (8.211.1)].

Theorem 1: The uplink ergodic rate from the kth user in the lth cell to its BS is given by

$$\langle R_{k} \rangle = \log_{2} e^{Q(\mathcal{A}_{l})} \sum_{n=1}^{\tau_{m}(\mathcal{A}_{l})} \sum_{p=0}^{N-K} \frac{\mathcal{X}_{m,n}(\mathcal{A}_{l}) \mu_{l,m}^{-n} (-1)^{N-K-p}}{(n-1)! (N-K-p)!} \left[-e^{\frac{1}{\beta_{llk}p_{u}}} \mathcal{I}_{n-1,N-K-p} \left(\frac{1}{\beta_{llk}}, \frac{1}{\beta_{llk}p_{u}}, \frac{1}{\mu_{l,m}} - \frac{1}{\beta_{llk}} \right) + \sum_{q=1}^{N-K-p} \frac{(q-1)! (-1)^{q} p_{u}^{-n}}{(\beta_{llk}p_{u})^{N-K-p-q}} \Gamma(n) U\left(n, n+N+1-K-p-q, \frac{1}{\mu_{l,m}p_{u}}\right) \right]$$
(14)

where $U(\cdot,\cdot,\cdot)$ is the confluent hypergeometric function of the second kind [30, Eq. (9.210.2)],

$$\mathcal{I}_{m,n}(a,b,\alpha) \triangleq \sum_{i=0}^{m} {m \choose i} (-b)^{m-i} \left[\sum_{q=0}^{n+i} \frac{(n+i)^q b^{n+i-q}}{\alpha^{q+1} a^{m-q}} \operatorname{Ei}(-b) - \frac{(n+i)^{n+i} e^{\alpha b/a}}{\alpha^{n+i+1} a^{m-n-i}} \operatorname{Ei}\left(-\frac{\alpha b}{a} - b\right) + \frac{e^{-b}}{\alpha} \sum_{q=0}^{n+i-1} \sum_{j=0}^{n+i-1} \frac{j! (n+i)^q {n+i-q-1 \choose j} b^{n+i-q-j-1}}{\alpha^q a^{m-q} (\alpha/a+1)^{j+1}} \right].$$
(15)

Proof: See Appendix A.

In practice, users are located randomly within cells, such that the large-scale fading factors for different users are different. This results in all diagonal elements of A_l being distinct. The following corollary corresponds to this practically important special case.

Corollary 1: If all diagonal elements of A_l are distinct, the ergodic rate in (14) reduces to

$$\langle R_k \rangle \! = \! \log_2 e \! \sum_{m=1}^{K(L\!-\!1)} \sum_{p=0}^{N\!-\!K} \frac{\prod_{n=1,n\neq m}^{K(L\!-\!1)} \left(1 - \mu_{l,n}/\mu_{l,m}\right)^{-1}}{\left(N\!-\!K\!-\!p\right)! \left(-1\right)^{N\!-\!K\!-\!p} \mu_{l,m}} \! \left[-e^{\frac{1}{\beta_{llk}p_{\mathrm{u}}}} \mathcal{I}_{0,N\!-\!K\!-\!p} \left(\! \frac{1}{\beta_{llk}}, \frac{1}{\beta_{llk}p_{\mathrm{u}}}, \frac{1}{\mu_{l,m}} \!-\! \frac{1}{\beta_{llk}} \! \right) \right] \!$$

$$+\sum_{q=1}^{N-K-p} \frac{(q-1)! (-1)^q}{\beta_{llk}^{N-K-p-q}} e^{\frac{1}{\mu_{l,m} p_{\mathbf{u}}}} \mu_{l,m}^{N+1-K-p-q} \Gamma\left(N+1-K-p-q, \frac{1}{\mu_{l,m} p_{\mathbf{u}}}\right)$$
(16)

where $\Gamma(a,x)=\int_x^\infty t^{a-1}e^{-t}dt$ being the upper incomplete gamma function [30, Eq. (8.350.2)].

Proof: For this case, substituting $\varrho(A_l) = K(L-1)$, $\tau_m(A_l) = 1$, and

$$\mathcal{X}_{m,1}\left(\mathcal{A}_{l}\right) = \prod_{n=1}^{K(L-1)} \left(1 - \frac{\mu_{l,n}}{\mu_{l,m}}\right)^{-1}$$

into (14), and using the identity $U(1, a, x) = e^x x^{1-a} \Gamma(a-1, x)$ [31, Eq. (07.33.03.0014.01)], we can obtain (16).

In addition to the exact result given by Theorem 1, we now derive an analytical lower bound on the ergodic achievable rate which is easier to evaluate:

Proposition 2: The uplink ergodic rate from the kth user in the lth cell to its BS is lower bounded by

$$\langle R_k \rangle \ge \log_2 \left(1 + p_{\mathbf{u}} \beta_{llk} \exp \left(\psi(N - K + 1) - p_{\mathbf{u}} \sum_{m=1}^{\varrho(\mathcal{A}_l)} \sum_{n=1}^{\tau_m(\mathcal{A}_l)} \mu_{l,m} n \mathcal{X}_{m,n} \left(\mathcal{A}_l \right) {}_{3}F_{1} \left(n + 1, 1, 1; 2; -p_{\mathbf{u}} \mu_{l,m} \right) \right) \right)$$

$$(17)$$

where $\psi(x)$ is Euler's digamma function [30, Eq. (8.360.1)], and ${}_{p}F_{q}(\cdot)$ represents the generalized hypergeometric function with p,q non-negative integers [30, Eq. (9.14.1)].

Remark 1: From (6), we have that

$$\lim_{p_{\mathbf{u}} \to \infty} \gamma_k \stackrel{\mathrm{d}}{=} \frac{X_k}{\sum_{i \neq l}^L \|\boldsymbol{Y}_i\|^2}.$$
 (18)

The above result explicitly demonstrates that the SINR is bounded when $p_{\rm u}$ goes to infinity. This means that at high SNRs, we cannot improve the system performance by simply increasing the

transmitted power of each user. The reason is that, when $p_{\rm u}$ increases, both the desired signal power and the interference power increase.

B. SER Analysis

In this section, we analyze the SER performance of the uplink for each user. Let $\mathcal{M}_{\gamma_k}(s)$ be the moment generating function (MGF) of γ_k . Then, using the well-known MGF-based approach [23], we can deduce the exact average SER of M-ary phase-shift keying (M-PSK) as follows:

Theorem 2: The average SER of the uplink from the kth user in the lth cell to its BS for M-PSK is given by

$$SER_k = \frac{1}{\pi} \int_0^{\Theta} \mathcal{M}_{\gamma_k} \left(\frac{g_{\text{MPSK}}}{\sin^2 \theta} \right) d\theta \tag{19}$$

where $\Theta \triangleq \pi - \frac{\pi}{M}$, $g_{\text{MPSK}} \triangleq \sin^2{(\pi/M)}$, and

$$\mathcal{M}_{\gamma_{k}}(s) = \sum_{m=1}^{\varrho(\mathcal{A}_{l})} \sum_{n=1}^{\tau_{m}(\mathcal{A}_{l})} \sum_{p=0}^{N-K+1} \binom{N-K+1}{p} \mathcal{X}_{m,n}(\mathcal{A}_{l}) \left(\frac{-\beta_{llk}s}{\beta_{llk}s + 1/p_{u}}\right)^{p} {}_{2}F_{0}\left(n, p; --; \frac{-\mu_{l,m}}{1/p_{u} + \beta_{llk}s}\right). \tag{20}$$

It is also interesting to investigate the SER at high SNRs in order to obtain the diversity gain of the system under consideration. For this case $(p_{\rm u} \to \infty)$, by ignoring $1/p_{\rm u}$ in (20), we obtain the asymptotic SER at high SNRs as

$$SER_k^{\infty} = \frac{1}{\pi} \int_0^{\Theta} \mathcal{M}_{\gamma_k}^{\infty} \left(\frac{g_{\text{MPSK}}}{\sin^2 \theta} \right) d\theta$$
 (21)

where

$$\mathcal{M}_{\gamma_{k}}^{\infty}(s) = \sum_{m=1}^{\varrho(\mathcal{A}_{l})} \sum_{n=1}^{\tau_{m}(\mathcal{A}_{l})} \sum_{n=0}^{N-K+1} \binom{N-K+1}{p} \mathcal{X}_{m,n}(\mathcal{A}_{l}) (-1)^{p} {}_{2}F_{0}\left(n, p; --; \frac{-\mu_{l,m}}{\beta_{llk}s}\right). \tag{22}$$

This implies that at high SNRs, the SER converges to a constant value that is independent of SNR; hence the diversity order, which is defined as $\lim_{p_u\to\infty}\frac{-\log \text{SER}_k}{\log(p_u)}$, is equal to zero. This phenomenon occurs due to the presence of interference. The following corollary corresponds to the interesting case when all diagonal elements of \mathcal{A}_l are distinct.

Corollary 2: If all diagonal elements of A_l are distinct, the exact and high-SNR MGF expressions in (20) and (22) reduce respectively to

$$\mathcal{M}_{\gamma_{k}}(s) = \sum_{m=1}^{K(L-1)} \sum_{p=0}^{N-K+1} {N-K+1 \choose p} \mathcal{X}_{m,1}(\mathcal{A}_{l}) \frac{(-\beta_{llk}s)^{p} \mu_{l,m}^{-1}}{(1/p_{u} + \beta_{llk}s)^{p-1}} e^{\frac{1/p_{u} + \beta_{llk}s}{\mu_{l,m}}} \mathbb{E}_{p} \left(\frac{1/p_{u} + \beta_{llk}s}{\mu_{l,m}} \right)$$
(23)

$$\mathcal{M}_{\gamma_{k}}^{\infty}(s) = \sum_{m=1}^{K(L-1)} \sum_{p=0}^{N-K+1} {N-K+1 \choose p} \mathcal{X}_{m,1}(\mathcal{A}_{l}) \frac{(-1)^{p} \beta_{llk} s}{\mu_{l,m}} e^{\frac{\beta_{llk} s}{\mu_{l,m}}} \mathbf{E}_{p} \left(\frac{\beta_{llk} s}{\mu_{l,m}}\right)$$
(24)

where $E_n(z) = \int_1^\infty t^{-n} e^{-zt} dt$, n = 0, 1, 2, ..., Re(z) > 0, is the exponential integral function of order n [31, Eq. (06.34.02.0001.01)].

Proof: Following a similar methodology as in Corollary 1 and using the identity

$$_{2}F_{0}(1, p; -; -x) = \frac{1}{x}e^{1/x}\mathbb{E}_{p}\left(\frac{1}{x}\right)$$
 (25)

we arrive at the desired results (23) and (24). Note that (25) is obtained by using [34, Eq. (8.4.51.1)], [34, Eq. (8.2.2.15)], [34, Eq. (8.4.16.14)] and [35, Eq. (46)].

From (19), we can see that to compute the SER we have to perform a finite integration over θ . To avoid this integration, we can apply the tight approximation of [32] on (19), to get

$$SER_{k} \approx \left(\frac{\Theta}{2\pi} - \frac{1}{6}\right) \mathcal{M}_{\gamma_{k}} \left(g_{MPSK}\right) + \frac{1}{4} \mathcal{M}_{\gamma_{k}} \left(\frac{4g_{MPSK}}{3}\right) + \left(\frac{\Theta}{2\pi} - \frac{1}{4}\right) \mathcal{M}_{\gamma_{k}} \left(\frac{g_{MPSK}}{\sin^{2}\Theta}\right). \tag{26}$$

Clearly, the above expression is easier to evaluate compared to (19).

C. Outage Probability Analysis

The main goal of this section is to analytically assess the outage probability of multicell MU-MIMO systems with ZF processing at the BS. Especially for the case of non-ergodic channels (e.g. quasi-static or block-fading), it is appropriate to resort to the notion of outage probability to characterize the system performance. The outage probability, P_{out} , is defined as the probability that the instantaneous SINR, γ_k , falls below a given threshold value γ_{th} , i.e.,

$$P_{\text{out}} \triangleq \Pr\left(\gamma_k \le \gamma_{\text{th}}\right).$$
 (27)

With this definition in hand, we can present the following novel, exact result:

Theorem 3: The outage probability of transmission from the kth user in the lth cell to its BS is given by

$$P_{\text{out}} = 1 - \exp\left(-\frac{\gamma_{\text{th}}}{p_{\text{u}}\beta_{llk}}\right)$$

$$\times \sum_{m=1}^{\varrho(\mathcal{A}_l)} \sum_{n=1}^{\tau_m(\mathcal{A}_l)} \sum_{p=0}^{N-K} \sum_{q=0}^{p} \binom{p}{q} \frac{\left(\frac{\gamma_{\text{th}}}{\beta_{llk}}\right)^p}{p!} \mathcal{X}_{m,n} \left(\mathcal{A}_l\right) \frac{\mu_{l,m}^{-n}}{(n-1)!} \frac{\Gamma\left(n+q\right) p_{\text{u}}^{q-p}}{\left(1/\mu_{l,m} + \gamma_{\text{th}}/\beta_{llk}\right)^{n+q}}. \tag{28}$$

Proof: See Appendix D.

Note that the exponential integral function and confluent hypergeometric functions appearing in Theorems 1, 2, and 3 are built in functions and can be easily evaluated by standard mathematical software packages, such as MATHEMATICA or MATLAB. We now recall that we are typically interested in small outage probabilities (e.g., in the order of 0.01, 0.001 etc). In this light, when $\gamma_{\rm th} \to 0$, we can obtain the following asymptotic result:

$$P_{\text{out}}^{\infty} = 1 - \sum_{m=1}^{\varrho(\mathcal{A}_l)} \sum_{n=1}^{\tau_m(\mathcal{A}_l)} \sum_{p=0}^{N-K} \frac{\left(\frac{\gamma_{\text{th}}}{\beta_{llk}}\right)^p}{p!} \mathcal{X}_{m,n}\left(\mathcal{A}_l\right) \frac{\mu_{l,m}^{-n}}{(n-1)!} \frac{\Gamma\left(n+p\right)}{\left(1/\mu_{l,m} + \gamma_{\text{th}}/\beta_{llk}\right)^{n+p}}.$$
 (29)

The above result is obtained by keeping the dominant term p=q in (28) and letting $\gamma_{\rm th}\to 0$. Similarly to the SER case, $P_{\rm out}^\infty$ is independent of the SNR, thereby reflecting the deleterious impact of interference. Furthermore, for the case described in Corollaries 1 and 2, we can get the following simplified results:

Corollary 3: If all diagonal elements of A_l are distinct, the exact and high-SNR outage probability expressions in (28) and (29) reduce respectively to

$$P_{\text{out}} = 1 - \exp\left(-\frac{\gamma_{\text{th}}}{p_{\text{u}}\beta_{llk}}\right) \sum_{m=1}^{K(L-1)} \sum_{p=0}^{N-K} \sum_{q=0}^{p} \frac{\left(\frac{\gamma_{\text{th}}}{\beta_{llk}}\right)^{p}}{(p-q)!} \frac{\mathcal{X}_{m,1}\left(\mathcal{A}_{l}\right)}{\mu_{l,m}} \frac{p_{\text{u}}^{q-p}}{(1/\mu_{l,m} + \gamma_{\text{th}}/\beta_{llk})^{q+1}}$$
(30)

$$P_{\text{out}}^{\infty} = 1 - \sum_{m=1}^{K(L-1)} \sum_{p=0}^{N-K} \left(\frac{\gamma_{\text{th}}}{\beta_{llk}}\right)^{p} \frac{\mathcal{X}_{m,1}(\mathcal{A}_{l})}{\mu_{l,m}} \frac{1}{(1/\mu_{l,m} + \gamma_{\text{th}}/\beta_{llk})^{1+p}}.$$
 (31)

IV. Asymptotic
$$(N \to \infty)$$
 Analysis

As discussed in Remark 1, we cannot improve the multicell MU-MIMO system performance by simply increasing the transmit power. However, we can improve the system performance by using a large number of BS antennas. Due to the array gain and diversity effects, when N increases, the received powers of both the desired and the interference signals increase. Yet,

based on the asymptotic orthogonal property of the channel vectors between the users and the BS, when N is large, the interference can be significantly reduced even with a simple ZF receiver [17], [19]. In this section, we analyze the asymptotic performance for large N. We assume that when N increases, the elements of the channel matrix are still independent. To guarantee the independence of the channels, the antennas have to be sufficiently well separated. Note that the physical size of the antenna array can be small even with very large N. For example, at 2.6 GHz, a cylindrical array with 128 antennas, which comprises 4 circles of 16 dual polarized antenna elements (distance between adjacent antennas is about 6 cm which is half a wavelength), occupies only a physical size of 28 cm \times 29 cm [24].

1) Fixed p_u , K, and $N \to \infty$: Intuitively, when the number of BS antennas N grows large, the random vectors between the BS and the users as well as the noise vector at the BS become pairwisely orthogonal and hence, the interference from other users can be cancelled out. At the same time, due to the array gain effect, thermal noise cancels out too. This intuition is confirmed by the following analysis.

Since X_k has an Erlang distribution with shape parameter N-K+1 and scale parameter β_{llk} , X_k can be represented as

$$X_k = \frac{\beta_{llk}}{2} \sum_{i=1}^{2(N-K+1)} Z_i^2 \tag{32}$$

where $Z_1, Z_2, ..., Z_{2(N-K+1)}$ are independent, standard normal RVs. Substituting (32) into (9), and dividing the denominator and the numerator of γ_k by 2(N-K+1), we obtain

$$\gamma_{k} = \frac{p_{u} \frac{\beta_{llk}}{2} \sum_{i=1}^{2(N-K+1)} Z_{i}^{2} / (2(N-K+1))}{\left(p_{u} \sum_{i\neq l}^{L} \|\boldsymbol{Y}_{i}\|^{2} + 1\right) / (2(N-K+1))} \stackrel{\text{a.s.}}{\to} \infty, \text{ as } N \to \infty$$
(33)

where (33) is obtained by using the law of large numbers, i.e., the numerator converges to $p_{\rm u}\beta_{llk}/2$, while the denominator converges to 0. The above result reveals that when the number of BS antennas goes to infinity, the effects of interference and noise disappear. Therefore, by increasing N, the SINR grows without limit. Similar conclusions were presented in [19].

2) Fixed p_u , $\kappa = N/K$, and $N \to \infty$: This is an interesting asymptotic scenario since in practice, the number of BS antennas, N, is large but may not be much greater than the number of users K. For this case, the property stating that the channel vectors between users and the BS are pairwisely orthogonal when $N \to \infty$ is not valid. In other words, $\mathbf{H}_{li}^H \mathbf{H}_{li}$ does not converge

point-wisely to an "infinite-size identity matrix" [18]. Therefore, the intercell interference cannot be cancelled out. Since $Y_i \sim \mathcal{CN}(\mathbf{0}, D_{li})$, it can be represented as

$$\boldsymbol{Y}_i = \boldsymbol{w}_i^H \boldsymbol{D}_{li}^{1/2} \tag{34}$$

where $w_i \sim \mathcal{CN}(\mathbf{0}, I_K)$. From (9), (32), and (34), γ_k can be expressed as

$$\gamma_k = \frac{p_{\rm u} \frac{\beta_{llk}}{2} \sum_{i=1}^{2(N-K+1)} Z_i^2}{p_{\rm u} \sum_{i \neq l}^{L} \mathbf{w}_i^H \mathbf{D}_{li} \mathbf{w}_i + 1}.$$
(35)

By dividing the numerator and denominator of γ_k in (35) by 2(N-K+1), we obtain

$$\gamma_{k} = \frac{p_{u} \frac{\beta_{llk}}{2} \sum_{i=1}^{2(N-K+1)} Z_{i}^{2} / (2(N-K+1))}{\left(p_{u} \sum_{i\neq l}^{L} \boldsymbol{w}_{i}^{H} \boldsymbol{D}_{li} \boldsymbol{w}_{i} + 1\right) / (2(N-K+1))}.$$
(36)

Since $N/K = \kappa$, $2(N - K + 1) = 2(N - \frac{1}{\kappa}N + 1) \to \infty$ as $N \to \infty$. Thus, by using the law of large numbers and the trace lemma from [25, Lemma 13], i.e.,

$$\frac{1}{K} \boldsymbol{w}_i^H \boldsymbol{D}_{li} \boldsymbol{w}_i - \frac{1}{K} \mathrm{Tr} \boldsymbol{D}_{li} \overset{\mathrm{a.s.}}{\rightarrow} 0, \text{ as } K \rightarrow \infty$$

we obtain

$$\gamma_k - \frac{\beta_{llk} (\kappa - 1)}{\sum_{i=1, i \neq l}^L \frac{1}{K} \operatorname{Tr} \mathbf{D}_{li}} \stackrel{\text{a.s.}}{\to} 0, \text{ as } N \to \infty, \text{ and } N/K = \kappa.$$
 (37)

Therefore a deterministic approximation, $\bar{\gamma}_k$, of γ_k is given by

$$\bar{\gamma}_k = \frac{\beta_{llk} \left(\kappa - 1\right)}{\sum_{i=1, i \neq l}^L \frac{1}{K} \text{Tr} \mathbf{D}_{li}}.$$
(38)

It is interesting to note that the SIR expression (38) is independent of the transmit power, and increases monotonically with κ . Therefore, for an arbitrarily small transmit power, the SIR (38) can be approached arbitrarily closely by using a sufficiently large number of antennas and users. The reason is that since the number of users K is large, the system is interference-limited, so if every user reduces its power by the same factor then the limiting SIR is unchanged. Furthermore, from (38), when $\kappa \to \infty$ (this is equivalent to the case $N \gg K$), the SIR $\bar{\gamma}_k \to \infty$, as $N \to \infty$, which is consistent with (33).

¹Note that the trace lemma holds if $\limsup_K \mathbb{E}\left\{\frac{1}{K} \text{Tr}\left(\boldsymbol{D}_{li}\boldsymbol{D}_{li}^H\right)^2\right\} < \infty$ which is equivalent to $\mathbb{E}\left\{\beta_{lik}^4\right\} < \infty$ [25, Remark 3]. For example, if β_{lik} is a log-normal random variable with standard deviation of σ , then $\mathbb{E}\left\{\beta_{lik}^4\right\} = e^{8\sigma^2}$ [26]. Evidently, for the vast majority of practical cases of interest, the standard deviation is finite, which makes the fourth moment bounded.

3) Fixed Np_u , $N \to \infty$: Let $p_u = E_u/N$, where E_u is fixed. From (33), we have

$$\gamma_k = \frac{E_{\mathbf{u}} \frac{\beta_{llk}}{2} \frac{\sum_{i=1}^{2(N-K+1)} Z_i^2}{2(N-K+1)} \frac{2(N-K+1)}{N}}{\frac{E_{\mathbf{u}}}{N} \sum_{i \neq l}^{L} \|\mathbf{Y}_i\|^2 + 1}.$$
(39)

Then, again using the law of large numbers and the trace lemma, we obtain

$$\gamma_k - \beta_{llk} E_u \stackrel{\text{a.s.}}{\to} 0,$$
 as $N \to \infty$, and fixed K (40)

$$\gamma_k - \frac{\beta_{llk} E_{\mathrm{u}} \left(1 - 1/\kappa \right)}{E_{\mathrm{u}}/\kappa \sum_{i=1, i \neq l}^{L} \frac{1}{K} \mathrm{Tr} \boldsymbol{D}_{li} + 1} \stackrel{\mathrm{a.s.}}{\to} 0, \text{ as } N \to \infty, N/K = \kappa.$$

$$(41)$$

These results show that by using a very large antenna array at the BS, we can cut the transmit power at each user proportionally to 1/N while maintaining a desired quality-of-service. This result was originally established in [19] for the case when $N\gg K\gg 1$ whereas herein, we have generalized this result to the regime where $N\gg 1$. Again, we can see that, when κ tends to infinity, the two asymptotic results (40) and (41) coincide.

Remark 2: We can see from (40) that when N grows without bound and K is fixed, the effects of interference and fast fading disappear. The only remaining effect is noise. Let us define the "massive MIMO effect" as the case where the system is ultimately limited by noise. From (41), when N grows large while keeping a finite κ , the system is still limited by interference from the other cells. This interference depends mainly on κ (the degrees of freedom), and when $\kappa \to \infty$, we operate under massive MIMO conditions. Therefore, an interesting question is: How many degrees of freedom κ are needed in order to make the interference small compared to the noise (i.e., to reach the massive MIMO condition)? Mathematically, we seek to find κ that satisfies

$$\log_2\left(1 + \frac{\beta_{llk}E_{\mathrm{u}}\left(1 - 1/\kappa\right)}{E_{\mathrm{u}}/\kappa\sum_{i=1, i \neq l}^L \frac{1}{K}\mathrm{Tr}\boldsymbol{D}_{li} + 1}\right) \ge \eta R_{k,\infty}, \text{ for a desired } \eta \in (0, 1)$$
 (42)

where $R_{k,\infty} = \log_2 (1 + \beta_{llk} E_u)$ is the ultimate rate which corresponds to the regime where $N \gg K \gg 1$. We more closely address this fundamental issue via simulations in Section V.

Remark 3: When $N \gg K \gg 1$ and $p_u = E_u/N$, using the property $\psi(x) = \ln(x) + 1/x + \mathcal{O}(1/x^2)$, and observing that the second term of the exponential function approaches zero, we

² The term "massive MIMO effect" was also used in [20] but in a different meaning, namely referring to the case when the system performance is limited by pilot contamination, due to the use of non-orthogonal pilots in different cells for the uplink training phase. However, here we assume perfect CSI, and we are considering a particular operating condition where the transmit power is very small $(p_{\rm u} \sim 1/N)$.

can simplify (17) to get $\langle R_k \rangle \ge \log_2 (1 + \beta_{llk} E_u)$, which coincides with (40). This implies that the proposed lower bound becomes exact in the large-number-of-antennas regime.

V. NUMERICAL RESULTS

In this section, we provide some numerical results to verify our analysis. Firstly, we consider a simple scenario where the large-scale fading is fixed. This setting enables us to validate the accuracy of our proposed analytical expressions as well as study the fundamental effects of intercell interference, number of BS antennas, transmit power of each user on the system performance. We then consider a more practical scenario that incorporates small-scale fading and large-scale fading including path-loss, shadowing, and random user locations.

A. Scenario I

We consider a multicell MU-MIMO system with 4 cells sharing the same frequency band. In all examples, except Fig. 4, we choose the number of users per cell to be K=10. We assume that all direct gains are equal to 1 and all cross gains are equal to a, i.e., $\beta_{llk}=1$, and $\beta_{ljk}=a, \forall j\neq l,\ k=1,2,...,K$ (a can be regarded as an interference factor). Furthermore, we define $\mathsf{SNR}\triangleq p_{\mathrm{u}}$.

Figure 1 shows the uplink sum rate per cell versus SNR, at cross gain a=0.1 and for different numbers of BS antennas $N=10,\ 20,\ 40,\ 60,\ 80$ and 100. The simulation curves are obtained by performing Monte-Carlo simulations using (5), while the analytical and bound curves are computed via (14) and (17), respectively. We can see that the simulated and analytical results match exactly. As expected, when N increases, the sum rate increases too. However, at high SNRs, the sum rate converges to a deterministic constant which verifies our analysis (18). Furthermore, a larger value of N makes the bound tighter. This is due to the fact that when N grows large, things that were random before become deterministic and hence, Jensen's inequality used in (51) will hold with equality (see Remark 3). Therefore, the bound can very efficiently approximate the rate when N is large. It can be also seen that, even for moderate number of antennas ($N \gtrsim 20$), the bound becomes almost exact across the entire SNR range.

The effect of interference for different N is shown in Fig. 2. Again, the simulated and analytical results match exactly, and the bound is very tight. Interestingly, its tightness does not depend on the interference level but on the number of BS antennas. We can see that when the cross gain increases (and hence, the interference increases), the sum rate decreases significantly. On the

other hand, the effect of interference decreases when the number of BS antennas grows large. For example, at a=0.1, the sum rates are 3.76, 38.35, and 73.20 for N=10, 50, and 500, respectively, while at a=0.5, the sum rates are respectively 0.93, 19.10, and 50.80 for N=10, 50, and 500. This means that when increasing the cross gain from 0.1 to 0.5, the sum rates are reduced by 75.27%, 50.20%, and 30.60% for N=10, 50, and 500, respectively.

The power efficiency of large array systems is investigated in Fig. 3. Figure 3 shows the uplink sum rate per cell versus N at $a=0.1,\ 0.3$, and 0.5 for the cases of $p_{\rm u}=10$ and $p_{\rm u}=10/N$. As expected, with $p_{\rm u}=10/N$, the sum rate converges to a constant value when N increases regardless of the effects of interference, and with $p_{\rm u}=10$, the sum rate grows without bound (logarithmically fast with N) when N increases (see (33) and (40)).

Figure 4 shows the required number of degrees of freedom κ to achieve 80% ($\eta=0.8$) and 90% ($\eta=0.9$) of a given ultimate rate $R_{k,\infty}$, for a=0.1, and a=0.5. We use (42) to determine κ . We can see that κ increases with $R_{k,\infty}$. Therefore, for multicell systems, the BS can serve more users with low data rates. This is due to the fact that when $R_{k,\infty}$ increases, the transmit power increases and hence, the interference also increases. Then, we need more degrees of freedom to mitigate interference. For the same reason, we can observe that when the interference factor a increases, the required κ increases as well.

In Fig. 5, the analytical SER curves are compared with the outputs of a Monte-Carlo simulation for different N. Here, we choose 4-PSK and a=0.1. The "Analytical (Exact)" curves are computed using Theorem 2, and the "Analytical (Approx)" curves are generated using (26). In addition, the high-SNR curves, generated via (21), are also overlaid. It can be easily observed that the analytical results coincide with the simulation results. Furthermore, we can see that the "Analytical (Approx)" curves are accurate in all cases. As in the analysis of the sum rate, when the SNR is moderately large, the SER decreases very slowly and approaches an error floor (the asymptotic SER) due to interference, when SNR grows large. Yet, we can improve the system performance by increasing the number of BS antennas. The effects of using large antenna arrays on the SER can be further verified in Fig. 6, where the SER is plotted as a function of N for different cross gains and 4-PSK, at SNR = 10 dB. We can see that the system performance improves systematically when we increase N.

B. Scenario II

We consider a hexagonal cellular network where each cell has a radius (from center to vertex) of 1000 meters. In each cell, K=10 users are located uniformly at random and we assume that no user is closer to the BS than $r_{\rm h}=100$ meters. The large-scale fading is modeled via $\beta_{lik}=z_{lik}/\left(r_{lik}/r_{\rm h}\right)^{\nu}$, where z_{lik} represents a log-normal RV with standard deviation of 8 dB, r_{lik} is the distance between the kth user in the ith cell to the lth BS, and ν is the path loss exponent. We choose $\nu=3.8$ for our simulations. Furthermore, we assume that the transmitted data is modulated using OFDM. Let $T_{\rm s}$ and $T_{\rm u}$ be the OFDM symbol duration and useful symbol duration, respectively. Then, we define the net uplink rate of the kth user in the lth cell as follows [17]:

$$R_k^{\text{net}} = \frac{B}{r} \frac{T_{\text{u}}}{T_{\text{s}}} \log_2 \left(1 + \frac{p_{\text{u}} X_k}{p_{\text{u}} Z_l + 1/r} \right)$$
(43)

where B is the total bandwidth, and r is the frequency-reuse factor. Note that (43) is obtained by using the result in Proposition 1. For our simulations, we choose parameters that resemble those of the LTE standard [17]: $T_{\rm s}=71.4\mu{\rm sec}$, and $T_{\rm s}=66.7\mu{\rm sec}$. We further assume that the total bandwidth of the system is 20 MHz. We neglect the effects of all users in all cells which are outside a circular region with a radius (from the lth BS) of 8000 meters. This is reasonable since the interference from all users which are outside this region is negligible due to the path loss.

Figure 7 shows the cumulative distribution of the net uplink rate per user for different frequency-reuse factors r=1, 3, and 7, and different number of BS antennas N=20,100. We can see that the number of BS antennas has a very strong impact on the performance. The probability that the net uplink rate is smaller than a given indicated rate decreases significantly when N increases. We consider the 95%-likely rates, i.e., the rate is greater than or equal to this indicated rate with probability 0.95. We can see that 95%-likely rates increase with N; for example, with frequency-reuse factor of 1, increasing the number of BS antennas from 20 to 100 yields a 8-fold improvement in the 95%-likely rate (from 0.170 Mbits/sec to 1.375 Mbits/sec). Furthermore, when N is large, the random channel becomes deterministic and hence, the probability that the uplink rate is around its mean becomes inherently higher.

When comparing the effects of using frequency-reuse factors, we can see that, at high rate (and hence at high SNR), smaller reuse factors are preferable, and vice versa at low rate. Furthermore,

we can observe that the gap between the performance of different reuse factors becomes larger when N increases. This is due to the fact that, when N is large, the intercell interference can be notably reduced; as a consequence, the bandwidth used has a larger impact on the system performance. Table I summarizes the 95%-likely net uplink rates as well as their mean values.

VI. CONCLUSION

In this paper, we analyzed in detail the uplink performance of data transmission from K single-antenna users in one cell to its N-antenna BS in the presence of interference from other cells. The BS uses ZF to detect the transmitted signals. We derived exact closed-form expressions for the most important figures of merit, namely the uplink rate, SER, and outage probability, assuming that the channel between the users and the BS is affected by Rayleigh fading, shadowing, and path loss.

Theoretically, when N increases we obtain array and diversity gains, which affect both the desired and interference signals. Hence, from this perspective the performance is not dramatically affected. However, since when the number of BS antennas is large, the channel vectors between the users and the BS are pairwisely asymptotically orthogonal, the interference can be cancelled out with a simple linear ZF receiver. As a consequence, by using a large antenna array, the performance of the multicell system improves significantly. Furthermore, we investigated the achievable power efficiency when using large antenna arrays at the BSs. Large antenna arrays enable us to reduce the transmitted power of each user proportionally to 1/N with no performance degradation, provided that the BS has perfect CSI. We further elaborated on the massive MIMO effect and the impact of frequency-reuse factors.

APPENDIX

A. Proof of Theorem 1

We first present the following lemma which is used to derive the closed-form expression of the achievable ergodic rate in Section III-A.

Lemma 1: Let $m, n \in \mathbb{N}$, $a, b \in \mathbb{R}$, and $\alpha \in \mathbb{R}^+$. Then

$$\int_0^\infty x^m (ax+b)^n e^{-\alpha x} \text{Ei} \left(-(ax+b)\right) dx = \mathcal{I}_{m,n} (a,b,\alpha)$$
(44)

where $\mathcal{I}_{m,n}(a,b,\alpha)$ is given by (15).

Proof: By applying the change of variables z = ax + b in (44), we have

$$\int_{0}^{\infty} x^{m} (ax+b)^{n} e^{-\alpha x} \operatorname{Ei} \left(-(ax+b)\right) dx = \frac{e^{\frac{\alpha b}{a}}}{a^{m+1}} \int_{b}^{\infty} (z-b)^{m} z^{n} e^{-\frac{\alpha z}{a}} \operatorname{Ei} \left(-z\right) dz$$

$$= \frac{e^{\frac{\alpha b}{a}}}{a^{m+1}} \sum_{i=0}^{m} {m \choose i} (-b)^{m-i} \mathcal{J}_{n+i} \left(b, \frac{\alpha}{a}\right)$$
(45)

where

$$\mathcal{J}_{p}(\alpha,\mu) \triangleq \int_{\alpha}^{\infty} z^{p} e^{-\mu z} \operatorname{Ei}(-z) dz, \quad \mu \geq 0.$$
 (46)

Using partial integration and the fact that $d\text{Ei}\left(z\right)/dz=e^{z}/z$, the integral (46) for $p\in\mathbb{N}$ can be evaluated as

$$\mathcal{J}_{p}(\alpha,\mu) = -\frac{e^{-\mu z}z^{p}}{\mu}\operatorname{Ei}(-z)\Big|_{\alpha}^{\infty} + \frac{1}{\mu}\int_{\alpha}^{\infty}e^{-\mu z}\left[pz^{p-1}\operatorname{Ei}(-z) + z^{p-1}e^{-z}\right]dz$$

$$= \mathcal{K}_{p}(\alpha,\mu) + \frac{p}{\mu}\mathcal{J}_{p-1}(\alpha,\mu) = \sum_{q=0}^{p-1}\left(\frac{p}{\mu}\right)^{q}\mathcal{K}_{p-q}(\alpha,\mu) + \left(\frac{p}{\mu}\right)^{p}\mathcal{J}_{0}(\alpha,\mu) \tag{47}$$

where the second equality follows from [30, Eq. (2.321.2)], where

$$\mathcal{K}_{p}(\alpha,\mu) \triangleq \frac{e^{-\alpha\mu}\alpha^{p}}{\mu} \operatorname{Ei}\left(-\alpha\right) + \frac{e^{-\alpha(\mu+1)}}{\mu} \sum_{q=0}^{p-1} \frac{q!\binom{p-1}{q}\alpha^{p-q-1}}{(\mu+1)^{q+1}}$$
(48)

while the last equality is obtained using recursion. Finally, by using [30, Eqs. (5.231.2) and (6.224.1)], $\mathcal{J}_0(\alpha, \mu)$ in (47) can be evaluated as

$$\mathcal{J}_0(\alpha,\mu) = -\frac{1}{\mu} \operatorname{Ei}\left(-\left(\mu+1\right)\alpha\right) + \frac{e^{-\alpha\mu}}{\mu} \operatorname{Ei}\left(-\alpha\right). \tag{49}$$

From (45), (47)–(49), we arrive at the desired result (44).

Using Lemma 1, and [33, Eq. (39)], we can easily obtain (14).

B. Proof of Proposition 2

From (12), the uplink ergodic rate from the kth user in the lth cell to its BS can be expressed as:

$$\langle R_k \rangle = \mathbb{E}_{X_k, Z_l} \left\{ \log_2 \left(1 + p_u \exp\left(\ln\left(\frac{X_k}{p_u Z_l + 1}\right) \right) \right) \right\}$$
 (50)

$$\geq \log_2\left(1 + p_{\mathbf{u}}\exp\left(\mathbb{E}_{X_k,Z_l}\left\{\ln\left(\frac{X_k}{p_{\mathbf{u}}Z_l + 1}\right)\right\}\right)\right) \tag{51}$$

$$= \log_2 (1 + p_u \exp (\mathbb{E}_{X_k} \{ \ln (X_k) \} - \mathbb{E}_{Z_l} \{ \ln (p_u Z_l + 1) \}))$$
 (52)

where we have exploited the fact that $\log_2(1 + \alpha \exp(x))$ is convex in x for $\alpha > 0$ along with Jensen's inequality. We can now evaluate the expectations in (52) and we begin with $\mathbb{E}_{X_k} \{\ln(X_k)\}$, which can be expressed as

$$\mathbb{E}_{X_k} \left\{ \ln(X_k) \right\} = \frac{\beta_{llk}^{-N+K-1}}{(N-K)!} \int_0^\infty \ln(x) e^{-x/\beta_{llk}} x^{N-K} dx = \psi(N-K+1) + \ln(\beta_{llk})$$
 (53)

where we have used [30, Eq. (4.352.1)] to evaluate the corresponding integral. The second expectation in (52) requires a different line of reasoning. In particular, we have that

$$\mathbb{E}_{Z_{l}}\left\{\ln\left(p_{u}Z_{l}+1\right)\right\} = \sum_{m=1}^{\varrho(\mathcal{A}_{l})} \sum_{n=1}^{\tau_{m}(\mathcal{A}_{l})} \mathcal{X}_{m,n}\left(\mathcal{A}_{l}\right) \frac{\mu_{l,m}^{-n}}{(n-1)!} \underbrace{\int_{0}^{\infty} \ln\left(p_{u}z+1\right) z^{n-1} e^{\frac{-z}{\mu_{l,m}}} dz}_{\triangleq \tau}.$$
 (54)

The integral \mathcal{I} admits the following manipulations

$$\mathcal{I} = \int_0^\infty G_{2,2}^{1,2} \left[p_{\mathbf{u}} z \, \middle| \, \begin{array}{c} 1,1\\1,0 \end{array} \right] z^{n-1} e^{\frac{-z}{\mu_{l,m}}} dz = \mu_{l,m}^n G_{3,2}^{1,3} \left[p_{\mathbf{u}} \mu_{l,m} \, \middle| \, \begin{array}{c} 1-n,1,1\\1,0 \end{array} \right]$$
(55)

where $G_{p,q}^{m,n}\left[x,\left|_{\beta_1,\ldots,\beta_q}^{\alpha_1,\ldots,\alpha_p}\right.\right]$ denotes the Meijer's-G function [30, Eq. (9.301)], and we have expressed the integrand $\ln(1+\alpha z)$ in terms of Meijer's-G function according to [34, Eq. (8.4.6.5)]. The final expression stems from [30, Eq. (7.813.1)]. In addition, we can simplify (55) as follows

$$\mathcal{I} = p_{\mathbf{u}} \mu_{l,m}^{n+1} G_{3,2}^{1,3} \left[p_{\mathbf{u}} \mu_{l,m} \middle| \begin{array}{c} -n,0,0 \\ 0,-1 \end{array} \right] = p_{\mathbf{u}} \mu_{l,m}^{n+1} \Gamma(n+1)_{3} F_{1} \left(n+1,1,1;2;-p_{\mathbf{u}} \mu_{l,m}\right)$$
(56)

where we have used [30, Eq. (9.31.5)] to obtain the first equality and [34, Eq. (8.4.51.1)] to obtain the second equality. Combining (54) with (56) and after some basic simplifications, we get

$$\mathbb{E}_{Z_{l}}\left\{\ln\left(p_{u}Z_{l}+1\right)\right\} = p_{u}\sum_{m=1}^{\varrho(\mathcal{A}_{l})}\sum_{n=1}^{\tau_{m}(\mathcal{A}_{l})}\mu_{l,m}n\mathcal{X}_{m,n}\left(\mathcal{A}_{l}\right){}_{3}F_{1}\left(n+1,1,1;2;-p_{u}\mu_{l,m}\right). \tag{57}$$

Substituting (53) and (57) into (52), we conclude the proof.

C. Proof of Theorem 2

The MGF of γ_k is given by

$$\mathcal{M}_{\gamma_k}(s) = \mathbb{E}_{\gamma_k} \left\{ e^{-s\gamma_k} \right\} = \int_0^\infty \mathbb{E}_{X_k} \left\{ e^{-s\gamma_k} \right\} p_{Z_l}(z) \, dz. \tag{58}$$

Using the PDF of X_k given by (7), we have that

$$\mathbb{E}_{X_k} \left\{ e^{-s\gamma_k} \right\} = \frac{1}{(N-K)! \beta_{llk}^{N-K+1}} \int_0^\infty x^{N-K} \exp\left(-x \left(\frac{1}{\beta_{llk}} + \frac{s}{z+1/p_u}\right)\right) dx$$

$$= \left(\frac{z+1/p_u}{z+1/p_u + \beta_{llk} s}\right)^{N-K+1}$$
(59)

where the last equality is obtained by using [30, Eq. (3.326.2)]. Substituting (59) into (58) and using (8), we get

$$\mathcal{M}_{\gamma_{k}}(s) = \int_{0}^{\infty} \sum_{m=1}^{\varrho(\mathcal{A}_{l})} \sum_{n=1}^{\tau_{m}(\mathcal{A}_{l})} \mathcal{X}_{m,n} \left(\mathcal{A}_{l}\right) \frac{\mu_{l,m}^{-n}}{(n-1)!} z^{n-1} e^{\frac{-z}{\mu_{l,m}}} \left(\frac{z+1/p_{u}}{z+1/p_{u}+\beta_{llk}s}\right)^{N-K+1} dz$$

$$= \sum_{m=1}^{\varrho(\mathcal{A}_{l})} \sum_{n=1}^{\tau_{m}(\mathcal{A}_{l})} \sum_{p=0}^{N-K+1} \binom{N-K+1}{p} \mathcal{X}_{m,n} \left(\mathcal{A}_{l}\right) \frac{(-1)^{p} \mu_{l,m}^{-n}}{(n-1)!} \left(\frac{\beta_{llk}s}{\beta_{llk}s+1/p_{u}}\right)^{p}$$

$$\times \int_{0}^{\infty} z^{n-1} e^{\frac{-z}{\mu_{l,m}}} \left(\frac{z}{1/p_{u}+\beta_{llk}s}+1\right)^{-p} dz \tag{60}$$

where the last equality is obtained by using the binomial expansion formula. To evaluate the integral in (60), we first express $\left(\frac{z}{1/p_u+\beta_{llk}s}+1\right)^{-p}$ in terms of a Meijer's-G function with the help of [30, Eq. (8.4.2.5)], and then using the identity [30, Eq. (2.24.3.1)] to obtain

$$\mathcal{M}_{\gamma_{k}}(s) = \sum_{m=1}^{\varrho(\mathcal{A}_{l})} \sum_{n=1}^{\tau_{m}(\mathcal{A}_{l})} \sum_{p=0}^{M-K+1} {N-K+1 \choose p} \mathcal{X}_{m,n}(\mathcal{A}_{l}) \frac{(-1)^{p}}{(n-1)!} \left(\frac{\beta_{llk}s}{\beta_{llk}s + 1/p_{u}} \right)^{p} \times \frac{1}{\Gamma(p)} G_{2,1}^{1,2} \left[\frac{\mu_{l,m}}{\beta_{llk}s + 1/p_{u}} \Big|_{0}^{1-n,1-p} \right].$$
(61)

Finally, using [34, Eq. (8.4.51.1)], we arrive at the desired result (20).

D. Proof of Theorem 3

From Proposition 1 and (27), we have

$$P_{\text{out}} \triangleq \Pr\left(\frac{X_k}{Z_l + 1/p_{\text{u}}} \le \gamma_{\text{th}}\right).$$
 (62)

We can now express the above probability in integral form as follows:

$$P_{\text{out}} = \int_0^\infty \Pr(X_k < \gamma_{\text{th}}(Z_\ell + 1/p_{\text{u}}) \mid Z_\ell) \, p_{Z_\ell}(z) dz. \tag{63}$$

The cumulative density function (CDF) of X_k can be shown to be equal to

$$F_{X_k}(x) = \Pr\left(X_k \le x\right) = 1 - \exp\left(-\frac{x}{\beta_{llk}}\right) \sum_{p=0}^{M-K} \frac{1}{p!} \left(\frac{x}{\beta_{llk}}\right)^p \tag{64}$$

where we have used the integral identity [30, Eq. (3.351.1)] to evaluate the CDF. Combining (63) with (64), we can rewrite P_{out} as follows:

$$P_{\text{out}} = \int_{0}^{\infty} \left(1 - \exp\left(-\frac{\gamma_{\text{th}}(z+1/p_{\text{u}})}{\beta_{llk}}\right) \sum_{p=0}^{N-K} \frac{1}{p!} \left(\frac{\gamma_{\text{th}}(z+1/p_{\text{u}})}{\beta_{llk}}\right)^{p}\right) p_{Z_{\ell}}(z) dz$$

$$= 1 - \exp\left(-\frac{\gamma_{\text{th}}}{p_{\text{u}}\beta_{llk}}\right) \sum_{p=0}^{N-K} \frac{1}{p!} \int_{0}^{\infty} \exp\left(-\frac{\gamma_{\text{th}}z}{\beta_{llk}}\right) \left(\frac{\gamma_{\text{th}}(z+1/p_{\text{u}})}{\beta_{llk}}\right)^{p} p_{Z_{\ell}}(z) dz$$

$$= 1 - \exp\left(-\frac{\gamma_{\text{th}}}{p_{\text{u}}\beta_{llk}}\right) \sum_{p=0}^{N-K} \frac{\left(\frac{\gamma_{\text{th}}}{\beta_{llk}}\right)^{p}}{p!} \int_{0}^{\infty} \exp\left(-\frac{\gamma_{\text{th}}z}{\beta_{llk}}\right) (1/p_{\text{u}} + z)^{p} p_{Z_{\ell}}(z) dz$$

$$= 1 - \exp\left(-\frac{\gamma_{\text{th}}}{p_{\text{u}}\beta_{llk}}\right) \sum_{m=1}^{\varrho(\mathcal{A}_{l})} \sum_{n=1}^{\tau_{m}(\mathcal{A}_{l})} \sum_{p=0}^{N-K} \frac{\left(\frac{\gamma_{\text{th}}}{\beta_{llk}}\right)^{p}}{p!} \mathcal{X}_{m,n} \left(\mathcal{A}_{l}\right) \frac{\mu_{l,m}^{-n}}{(n-1)!}$$

$$\times \int_{0}^{\infty} (1/p_{\text{u}} + z)^{p} z^{n-1} \exp\left(-z\left(\frac{1}{\mu_{l,m}} + \frac{\gamma_{\text{th}}}{\beta_{llk}}\right)\right) dz. \quad (65)$$

Using the binomial expansion and [30, Eq. (3.326.2)], we arrive at the desired result (28).

REFERENCES

- [1] H. Q. Ngo, T. Q. Duong, and E. G. Larsson, "Uplink performance analysis of multicell MU-MIMO with zero-forcing receivers and perfect CSI," in *Proc. IEEE Swedish Commun. Techn. Work. (Swe-CTW)*, Stockholm, Sweden, Nov. 2011, pp. 40–45.
- [2] D. Gesbert, M. Kountouris, R. W. Heath Jr., C.-B. Chae, and T. Sälzer, "Shifting the MIMO paradigm," *IEEE Signal Process. Mag.*, vol. 24, no. 5, pp. 36–46, Sep. 2007.
- [3] L.-U. Choi and R. D. Murch, "A transmit preprocessing technique for multiuser MIMO systems using a decomposition approach," *IEEE Trans. Wireless Commun.*, vol. 3, no. 1, pp. 20–24, Jan. 2004.
- [4] N. Jindal and A. Goldsmith, "Dirty-paper coding versus TDMA for MIMO broadcast channels," *IEEE Trans. Inf. Theory*, vol. 51, no. 5, pp. 1783–1794, May 2005.
- [5] S. Verdú, Multiuser Detection. Cambridge, UK: Cambridge University Press, 1998.
- [6] M. Matthaiou, N. D. Chatzidiamantis, G. K. Karagiannidis, and J. A. Nossek, "ZF detectors over correlated *K* fading MIMO channels," *IEEE Trans. Commun.*, vol. 59, no. 6, pp. 1591–1603, Jun. 2011.
- [7] C.-J. Chen and L.-C. Wang, "Performance analysis of scheduling in multiuser MIMO systems with zero-forcing receivers," *IEEE J. Sel. Areas Commun.*, vol. 25, no. 7, pp. 1435–1445, Sep. 2007.
- [8] A. Forenza, M. R. McKay, A. Pandharipande, R. W. Heath Jr., and I. B. Collings, "Adaptive MIMO transmission for exploiting the capacity of spatially correlated channels," *IEEE Trans. Veh. Technol.*, vol. 56, no. 2, pp. 619–630, Mar. 2007.
- [9] S. Catreux, P. F. Driessen, and L. J. Greenstein, "Simulation results for an interference-limited multiple-input multiple-output cellular system," *IEEE Commun. Lett.*, vol. 4, no. 11, pp. 334–336, Feb. 2000.
- [10] R. S. Blum, "MIMO capacity with interference," IEEE J. Sel. Areas Commun., vol. 21, no. 5, pp. 798-801, Nov. 2003.

- [11] H. Dai, A. F. Molisch, and H. V. Poor, "Downlink capacity of interference-limited MIMO systems with joint detection," *IEEE Trans. Wireless Commun.*, vol. 3, no. 2, pp. 798–801, Mar. 2004.
- [12] D. Gesbert, S. V. Hanly, H. Huang, S. Shamai (Shitz), O. Simeone, and W. Yu, "Multi-cell MIMO cooperative networks: A new look at interference," *IEEE J. Sel. Areas Commun.*, vol. 28, no. 9, pp. 1380–1408, Dec. 2010.
- [13] J. Jose, A. Ashikhmin, T. L. Marzetta, and S. Vishwanath, "Pilot contamination and precoding in multi-cell TDD systems," *IEEE Trans. Wireless Commun.*, vol. 10, no. 8, pp. 2640–2651, Aug. 2011.
- [14] W. Choi and J. G. Andrews, "The capacity gain from intercell scheduling in muti-antenna systems," *IEEE Trans. Wireless Commun.*, vol. 7, no. 2, pp. 714–725, Feb. 2008.
- [15] C. Suh, M. Ho, and D. N. C. Tse, "Downlink interference alignment," *IEEE Trans. Commun.*, vol. 59, no. 9, pp. 2616–2626, Sep. 2011.
- [16] F. Rusek, D. Persson, B. K. Lau, E. G. Larsson, T. L. Marzetta, O. Edfors, and F. Tufvesson, "Scaling up MIMO: Opportunities and challenges with very large arrays," *IEEE Signal Process. Mag.*, to appear. [Online]. Available: http://arxiv.org/abs/1201.3210.
- [17] T. L. Marzetta, "Noncooperative cellular wireless with unlimited numbers of base station antennas," *IEEE Trans. Wireless Commun.*, vol. 9, no. 11, pp. 3590–3600, Nov. 2010.
- [18] R. Couillet and M. Debbah, "Signal processing in large systems: A new paradigm," *IEEE Signal Process. Mag.*, submitted. [Online]. Available: http://arxiv.org/abs/1105.0060.
- [19] H. Q. Ngo, E. G. Larsson, and T. L. Marzetta, "Energy and spectral efficiency of very large multiuser MIMO systems," *IEEE Trans. Commun.*, submitted. [Online]. Available: http://arxiv.org/abs/1112.3810.
- [20] J. Hoydis, S. ten Brink, and M. Debbah, "Massive MIMO: How many antennas do we need?" in *Proc. 49th Allerton Conference on Communication, Control, and Computing*, Urbana-Champaign, IL, Sep. 2011.
- [21] M. R. McKay, I. B. Collings, and A. M. Tulino, "Achievable sum rate of MIMO MMSE receivers: A general analytic framework," *IEEE Trans. Inf. Theory*, vol. 56, no. 1, pp. 396–410, Jan. 2010.
- [22] D. N. C. Tse and P. Viswanath, *Fundamentals of Wireless Communications*. Cambridge, UK: Cambridge University Press, 2005.
- [23] M. K. Simon and M.-S. Alouini, Digital Communication over Fading Channels: A Unified Approach to Performance Analysis. New York: Wiley, 2000.
- [24] X. Gao, O. Edfors, F. Rusek, and F. Tufvesson, "Linear pre-coding performance in measured very-large MIMO channels," in *Proc. IEEE Veh. Technol. Conf. (VTC)*, San Francisco, CA, Sept. 2011.
- [25] J. Hoydis, "Random matrix methods for advance communication systems," Ph.D. dissertation, SUPELEC, France, April 2012.
- [26] S. C. Schwartz and Y. S. Yeh, "On the distribution function and moments of power sums with log-normal components," *Bell Syst. Tech. J.*, vol. 61, no. 7, Sept. 1982.
- [27] H. Shin and M. Z. Win, "MIMO diversity in the presence of double scattering," *IEEE Trans. Inf. Theory*, vol. 54, no. 7, pp. 2976–2996, Jul. 2008.
- [28] D. A. Gore, R. W. Heath Jr., and A. J. Paulraj, "Transmit selection in spatial multiplexing systems," *IEEE Commun. Lett.*, vol. 6, no. 11, pp. 491–493, Nov. 2002.
- [29] A. Bletsas, H. Shin, and M. Z. Win, "Cooperative communications with outage-optimal opportunistic relaying," *IEEE Trans. Wireless Commun.*, vol. 6, no. 9, pp. 3450–3460, Sep. 2007.
- [30] I. S. Gradshteyn and I. M. Ryzhik, Table of Integrals, Series, and Products, 7th ed. San Diego, CA: Academic, 2007.

- [31] Wolfram, "The Wolfram functions site." Available: http://functions.wolfram.com
- [32] M. R. McKay, A. Zanella, I. B. Collings, and M. Chiani, "Error probability and SINR analysis of optimum combining in Rician fading," *IEEE Trans. Commun.*, vol. 57, no. 3, pp. 676–687, Mar. 2009.
- [33] M. Kang and M.-S. Alouini, "Capacity of MIMO Rician channels," *IEEE Trans. Wireless Commun.*, vol. 5, no. 1, pp. 112–122, Jan. 2006.
- [34] A. P. Prudnikov, Y. A. Brychkov, and O. I. Marichev, *Integrals and Series, Volume 3: More Special Functions*. New York: Gordon and Breach Science, 1990.
- [35] H. Shin and J. H. Lee, "Capacity of multiple-antenna fading channels: Spatial fading correlation, double scattering, and keyhole," *IEEE Trans. Inf. Theory*, vol. 49, no. 10, pp. 2636-2647, Oct. 2003.

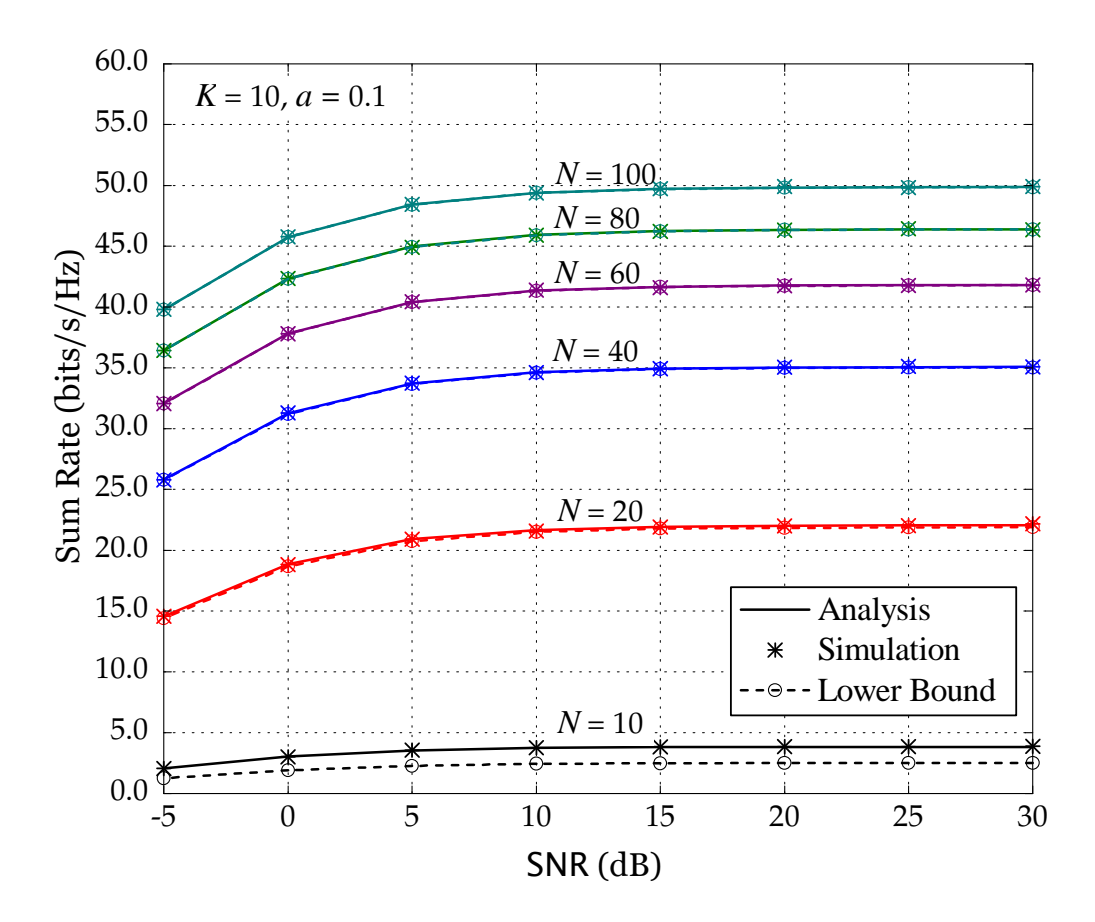


Fig. 1. Simulated uplink sum rate, analytical expression and lower bound versus the SNR ($L=4,\,K=10$, and a=0.1).

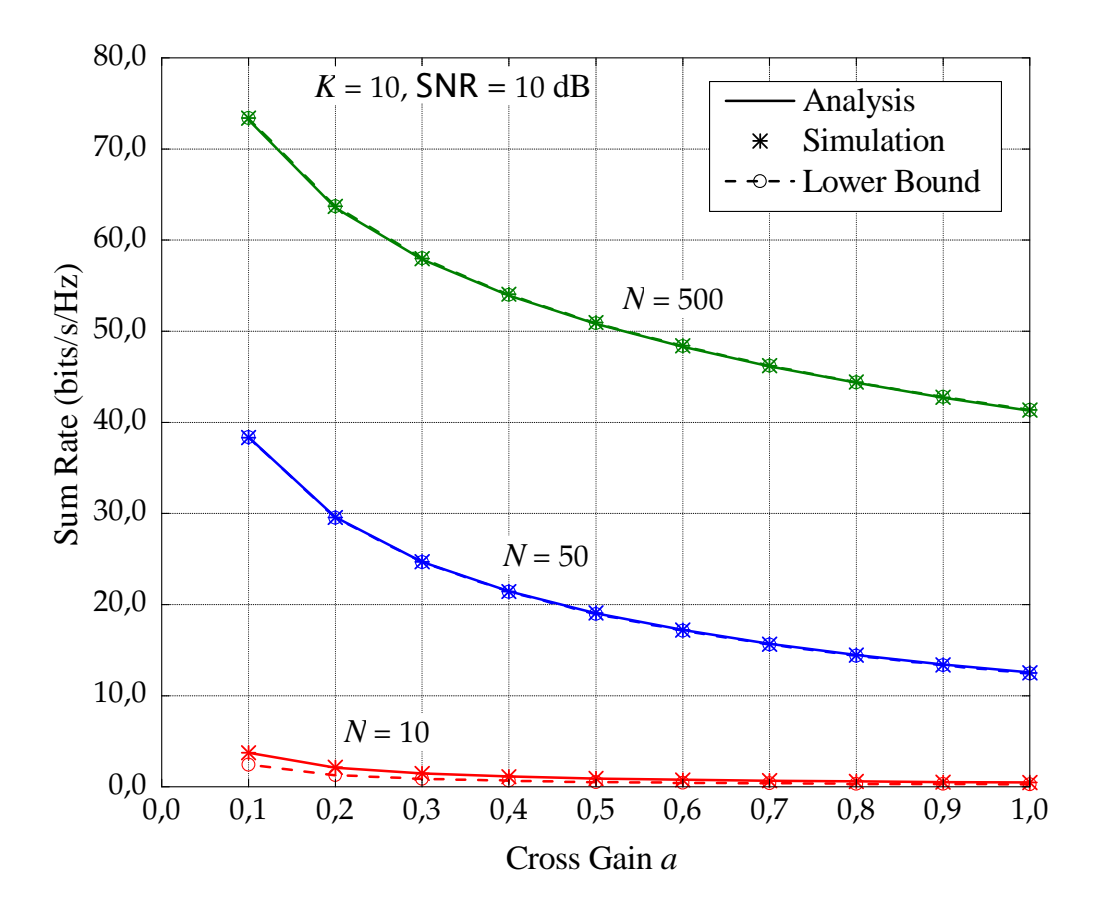


Fig. 2. Simulated uplink sum rate, analytical expression and lower bound versus the cross gain a (L=4, K=10, and SNR=10 dB).

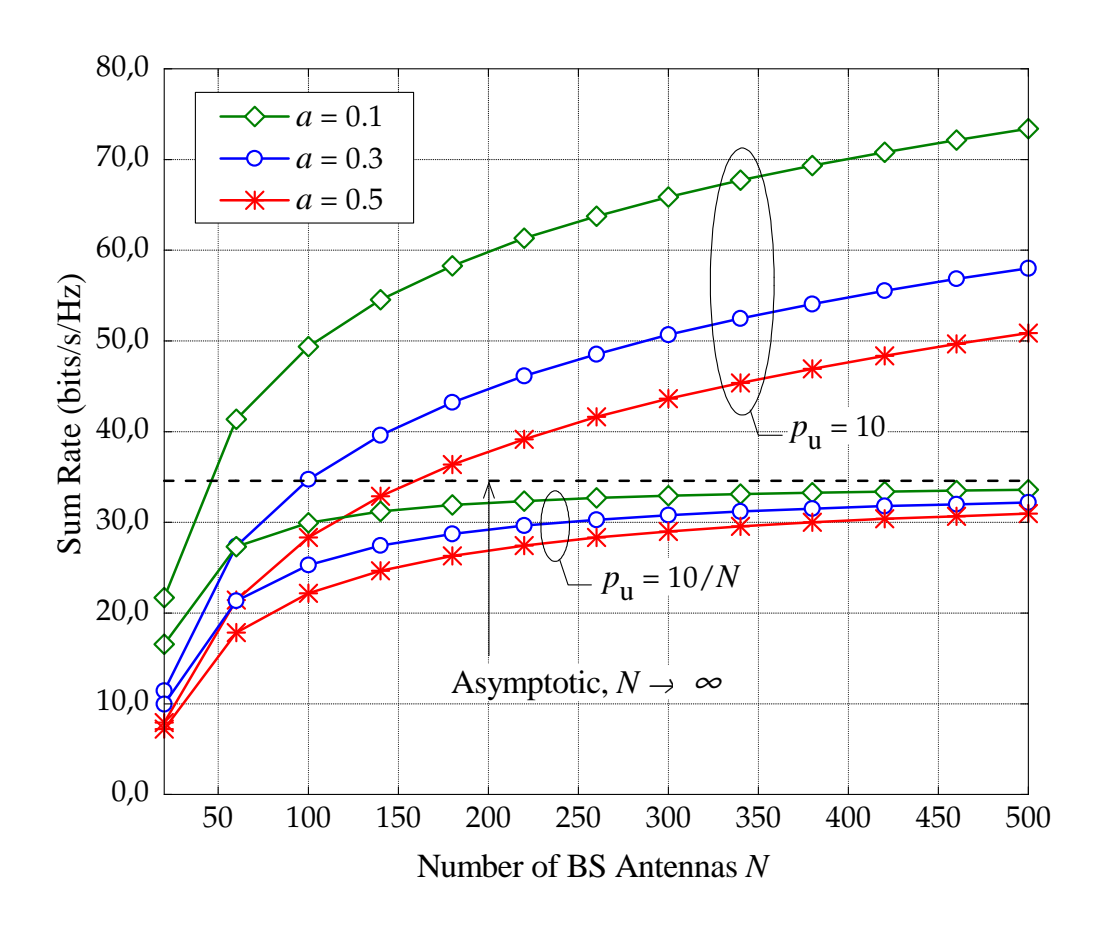


Fig. 3. Analytical uplink sum rate versus the number of BS antennas N ($L=4,\ K=10,\ a=0.1,\ 0.3,\ {\rm and}\ 0.5$).

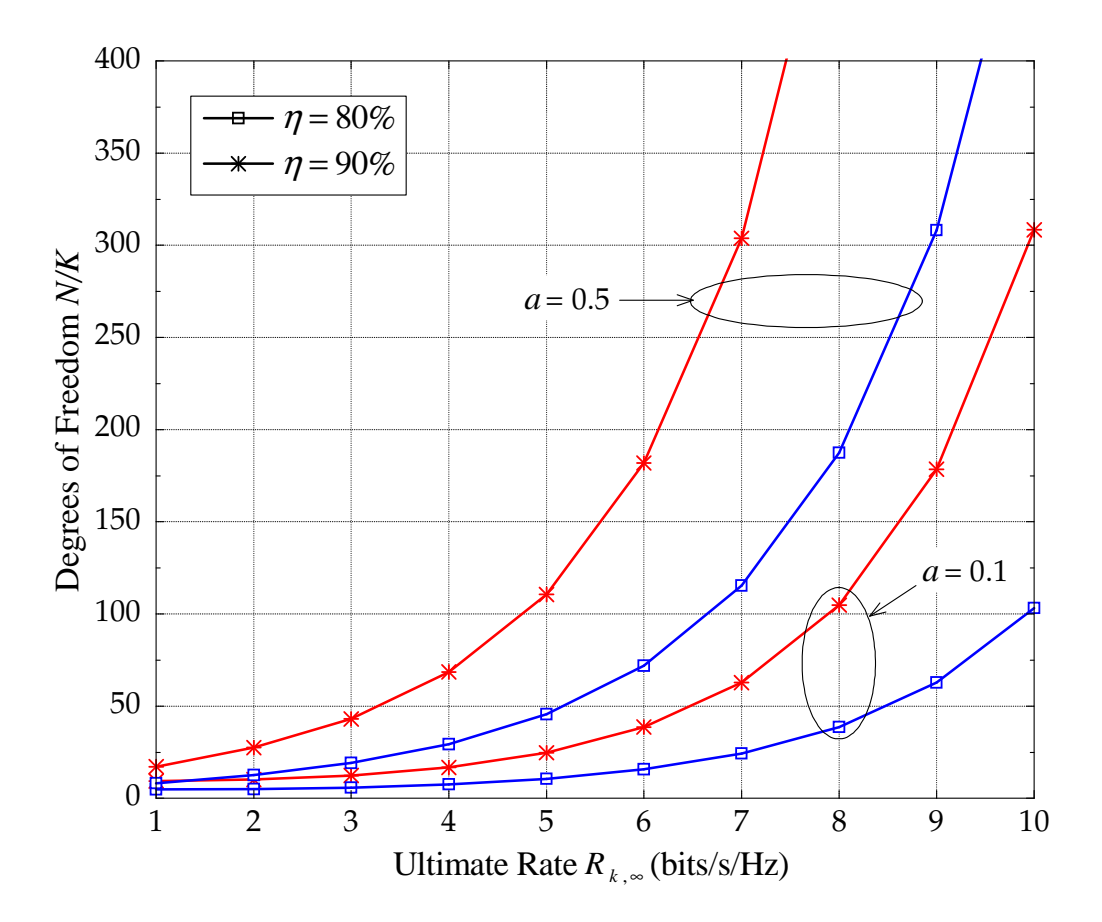


Fig. 4. Degrees of freedom κ required to achieve $\eta R_{k,\infty}$ versus $R_{k,\infty}$ (L=4,~a=0.1 and 0.5).

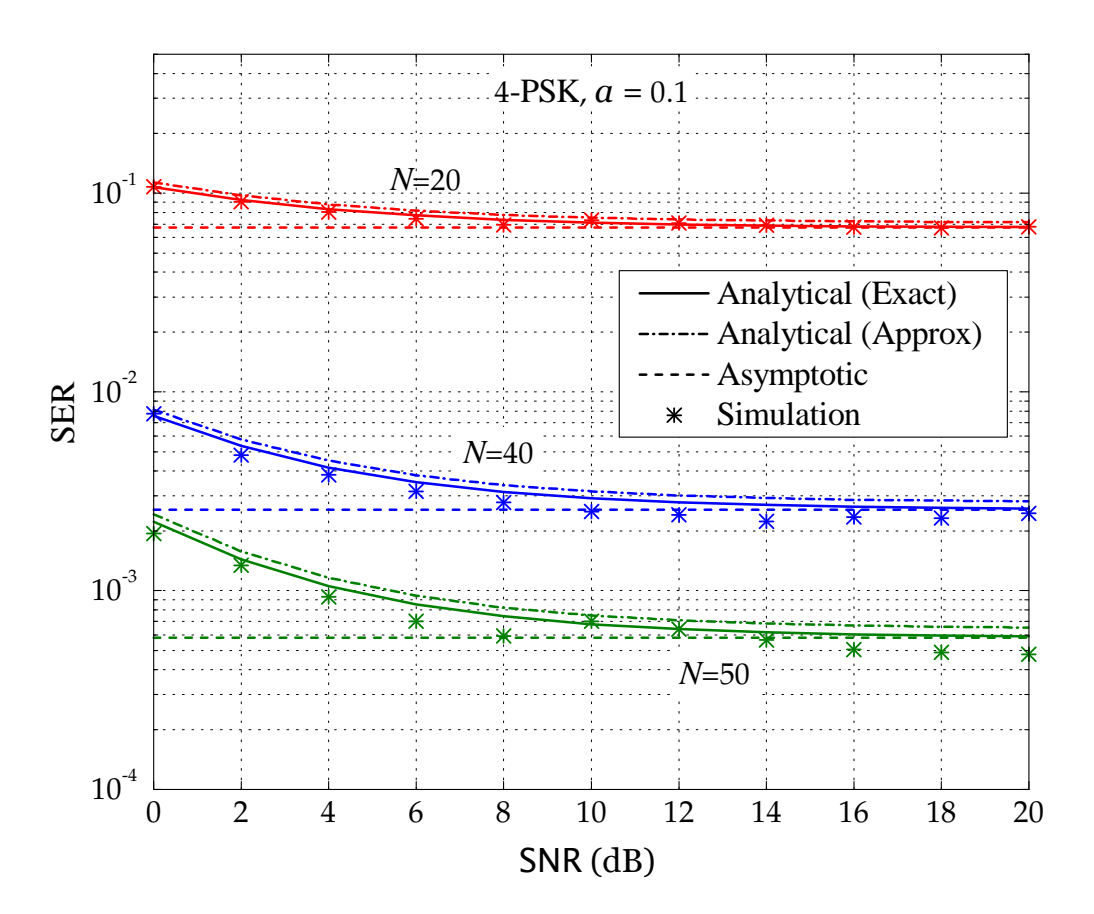


Fig. 5. Simulated average SER and analytical expression versus the SNR for 4-PSK ($L=4,\,K=10$ and a=0.1).

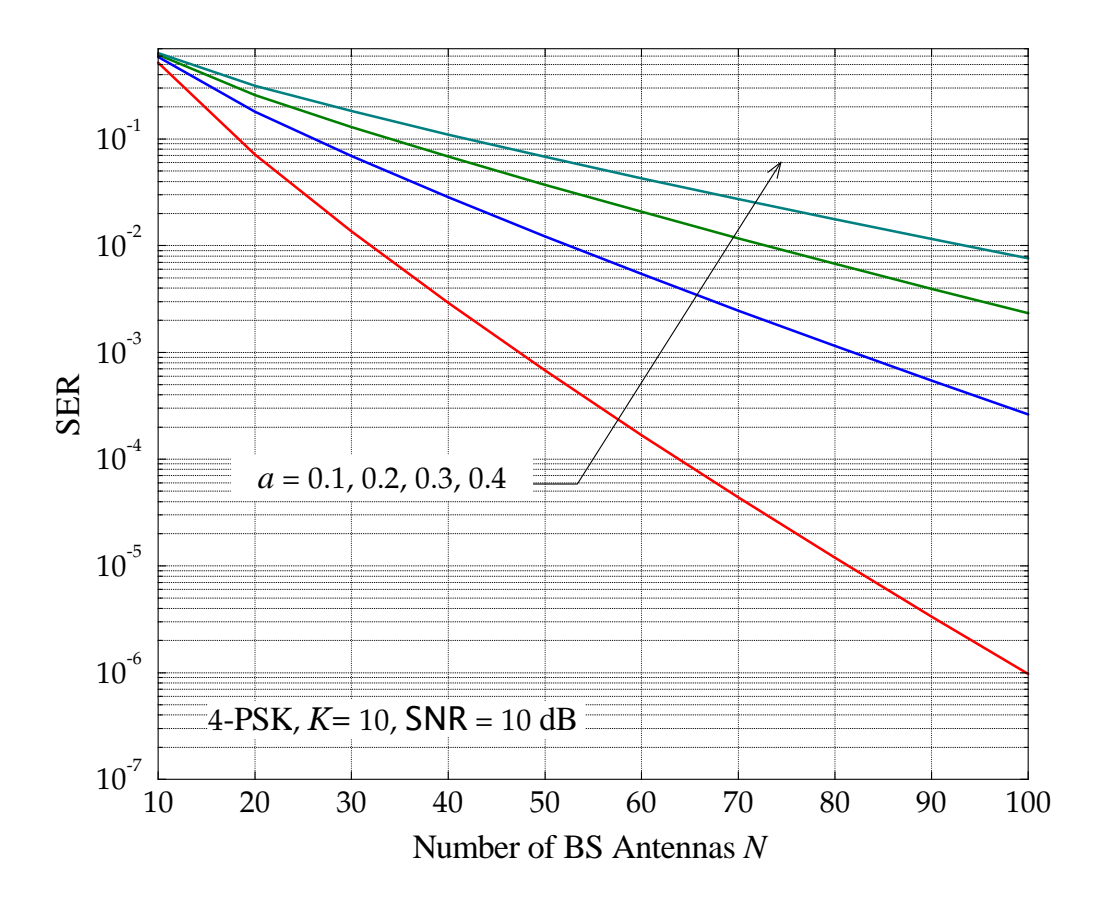


Fig. 6. Analytical average SER versus the number of BS antennas N (L=4, K=10, a=0.1, 0.2, 0.3, and 0.4).

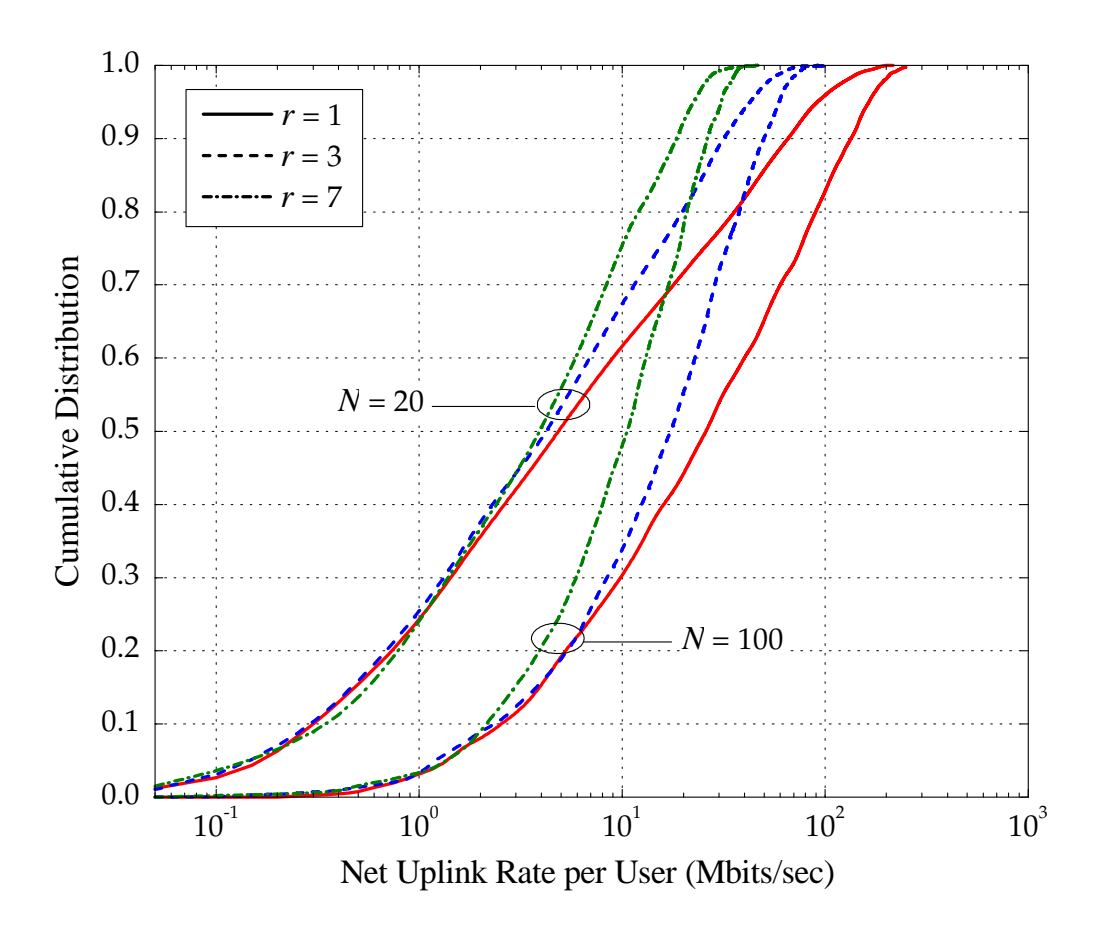


Fig. 7. Cumulative distribution of the net uplink rate per user for frequency-reuse factors 1, 3, and 7 ($N=20,\,100,\,$ SNR =10 dB, $\sigma_{\rm shadow}=8$ dB, and $\nu=3.8$).

TABLE I $\mbox{Uplink performance of ZF with frequency-reuse factors 1, 3, and 7, for } p_{\rm u}=10 \mbox{dB}, N=20, 100,$ $\sigma_{\rm shadow}=8 \mbox{dB}, \mbox{and } \nu=3.8$

Frequency Reuse Factor	0.95-likely Net Uplink Rate per User (Mbits/sec)		Mean of the Net Uplink Rate per User (Mbits/sec)	
	N=20	<i>N</i> =100	N=20	N=100
1	0.170	1.375	20.295	48.380
3	0.150	1.205	10.668	21.945
7	0.145	1.350	6.731	12.546